

Spray Dried Aerosol Particles of Pyrazinoic Acid Salts for Tuberculosis Therapy

Phillip Durham, Yanan Zhang, Nadezhda German, Ninell Pollas Mortensen, Jasvir Dhillon, Denis Anthony Mitchison, Petreus Bernard Fourie, and Tony Hickey

Mol. Pharmaceutics, **Just Accepted Manuscript** • DOI: 10.1021/acs.molpharmaceut.5b00118 • Publication Date (Web): 22 Jun 2015

Downloaded from <http://pubs.acs.org> on June 29, 2015

Just Accepted

“Just Accepted” manuscripts have been peer-reviewed and accepted for publication. They are posted online prior to technical editing, formatting for publication and author proofing. The American Chemical Society provides “Just Accepted” as a free service to the research community to expedite the dissemination of scientific material as soon as possible after acceptance. “Just Accepted” manuscripts appear in full in PDF format accompanied by an HTML abstract. “Just Accepted” manuscripts have been fully peer reviewed, but should not be considered the official version of record. They are accessible to all readers and citable by the Digital Object Identifier (DOI®). “Just Accepted” is an optional service offered to authors. Therefore, the “Just Accepted” Web site may not include all articles that will be published in the journal. After a manuscript is technically edited and formatted, it will be removed from the “Just Accepted” Web site and published as an ASAP article. Note that technical editing may introduce minor changes to the manuscript text and/or graphics which could affect content, and all legal disclaimers and ethical guidelines that apply to the journal pertain. ACS cannot be held responsible for errors or consequences arising from the use of information contained in these “Just Accepted” manuscripts.



1
2
3
4
5
6
7
8
9
10
11
12
13
14
15
16
17
18
19
20
21
22
23
24
25
26
27
28
29
30
31
32
33
34
35
36
37
38
39
40
41
42
43
44
45
46
47
48
49
50
51
52
53
54
55
56
57
58
59
60

Spray Dried Aerosol Particles of Salts for Tuberculosis Therapy

P.G. Durham¹, Y. Zhang¹, N. German^{1,2}, N. Mortensen¹, J. Dhillon³, D.A. Mitchison³,
P.B. Fourie⁴ and A.J. Hickey^{1*}

¹RTI International, Research Triangle Park, NC27709, USA,

²Currently, School of Pharmacy, Texas Tech. University Health Sciences Center,
Amarillo, TX79106, USA

³St George's Hospital, University of London, UK

⁴Department of Medical Microbiology, University of Pretoria, South Africa,

*Author for correspondence

ABSTRACT

1
2
3
4
5
6
7 Tuberculosis is the most serious infectious disease caused by a single organism,
8
9 *Mycobacterium tuberculosis* (*Mtb*). The standard of care is a protracted and complex
10
11 drug treatment regimen made more complicated and of longer duration by the incidence
12
13 of multiple- and extensively drug resistant disease. Pulmonary delivery of aerosols as a
14
15 supplement to the existing regimen offers the advantage of delivering high local drug
16
17 doses to the initial site of infection and most prominent organ system involved in
18
19 disease. Pyrazinamide is used in combination with other drugs to treat tuberculosis. It is
20
21 postulated that the action of pyrazinoic acid (POA), the active moiety of pyrazinamide,
22
23 may be enhanced by local pH adjustment, when presented as a salt form. POA was
24
25 prepared as leucine (POA-leu) and ammonium salts (POA-NH₄), spray dried and
26
27 characterized in terms of physico-chemical properties (melting point, crystallinity,
28
29 moisture content), aerodynamic performance (aerodynamic particle size distribution,
30
31 emitted dose) and in vitro inhibitory effect on two mycobacteria (*Mtb* and *Mycobacterium*
32
33 *bovis*) . Particles were prepared in sizes suitable for inhalation (3.3 and 5.4 μ m mass
34
35 median aerodynamic diameter and 61 and 40% of the aerodynamic particle size
36
37 distribution less than 4.46 μ m, as measured by inertial impaction, for POA-leu and POA-
38
39 NH₄, respectively) and with properties (stoichiometric 1:1 ratio of salt to drug, melting
40
41 points at ~180°C, with water content of <1%) that would support further development as
42
43 an inhaled dosage form. In addition, POA salts demonstrated greater potency in
44
45 inhibiting mycobacterial growth compared with POA alone which is promising for
46
47 therapy.
48
49
50
51
52
53
54
55
56
57
58
59
60

INTRODUCTION

1
2
3
4
5
6
7 More than 9 million cases of tuberculosis (TB), with 1.5 million deaths, occur each year
8
9 [1] despite the availability of effective treatment. The standard of care for TB in most
10
11 high-burden regions is a six month regimen, in which the initial 2 months include
12
13 isoniazid (INH), rifampicin (RIF), pyrazinamide (PZA) and ethambutol (E), followed by a
14
15 4 month continuation phase of RIF and INH (underlined letters used as abbreviations for
16
17 courses shown below). The introduction of RIF and PZA into TB therapy allowed the
18
19 duration of treatment to be reduced from at least 12 months to 6 months with <5%
20
21 relapses. However, further reductions in the duration of treatment resulted in increasing
22
23 rates of relapse after completion of treatment [2]. In the absence of a new more
24
25 efficacious regimen, there is general agreement that shortening the duration of
26
27 treatment with the current regimen from 6 months to 3 months or less would be a useful
28
29 improvement since it would reduce the burden of lengthy treatment and the supervision
30
31 of drug-taking for the patients and for the clinic, as well as diminishing the emergence of
32
33 drug resistance. Indeed, at a recent meeting of the TB Union the importance of
34
35 shortening the duration of therapy was identified [3]. While we wait for the advent of
36
37 affordable new drugs, a way forward to improve the efficacy of treatment of pulmonary
38
39 TB and shortening its duration is to improve the performance of the two drugs, RIF and
40
41 PZA, that are together responsible for almost all of the bactericidal action of the
42
43 2EHRZ/4RH regimen [4]. The subject of PZA in TB therapy has recently become the
44
45 focus for discussion and exploration, providing a rationale for the studies described here
46
47 [3, 5-8].
48
49
50
51
52
53
54
55
56
57
58
59
60

1
2
3 Tuberculosis is acquired by entry of *Mycobacterium tuberculosis* (*Mtb*) by the
4 pulmonary route. In addition, throughout disease progression the lung is a primary site
5 of infection. Upon deposition in the lungs infectious organisms are taken up by
6 macrophages as depicted in Figures 1a and b. The mechanism of action of PZA and
7 POA should be considered in order to characterize the outcome of lung delivery with
8 respect to treatment of infection.
9
10
11
12
13
14
15
16

17
18 PZA was introduced by Lederle and Merck [9, 10] in the early 1950s as a result
19 of its high activity in experimental murine TB. Following a small clinical study on its use
20 in treating patients [11, 12], it was then studied at Cornell University using the long term
21 mouse model [12]. Mice were infected and treated with a combination of PZA with INH,
22 to prevent rapid emergence of PZA resistance [13]. As treatment progressed, counts of
23 viable *M. tuberculosis* in the spleens of mice treated with INH+PZA decreased in
24 parallel to the counts on the control mice treated with INH, streptomycin, and p-
25 aminosalicylic acid (PAS) for the first 2-3 weeks, but continued downwards eventually to
26 no colonies on culture while the counts on the control culture gradually decreased to a
27 constant proportion of surviving persisters. Further clinical development of pyrazinamide
28 showed that at appropriate doses, PZA could substantially accelerate the progress of
29 chemotherapy [14].
30
31
32
33
34
35
36
37
38
39
40
41
42
43
44
45
46

47 PZA was shown in 1967 to be a pro-drug that was converted to the active
48 molecule POA by the amidase of *M. tuberculosis* [15]. POA itself was not absorbed from
49 the gastrointestinal tract (GI). A more detailed description of the mode of action of PZA
50 has been provided recently by Zhang who had access to labeled PZA and could,
51 therefore, track the movement of PZA and POA within and in the immediate
52
53
54
55
56
57
58
59
60

1
2
3 surroundings of the bacilli [16]. In a series of publications, Zhang developed a
4
5 hypothesis illustrated in Figure 1d. In this, the PZA is first de-aminated within the
6
7 cytoplasm of *Mtb* -being converted to $-NH_3$ and POA by the amidase *pncA* [17]. The
8
9 POA then leaves the bacterial cell and, if the local environment is acidic, re-enters the
10
11 cell by passive diffusion in a highly pH dependent manner according to the Henderson-
12
13 Hasselbach equation. Once in the cell, the POA can only escape with the help of an
14
15 inefficient, energy dependent, efflux pump. Thus, if there is only a small energy pool
16
17 available to run the inefficient pump, POA will tend to accumulate within the cell and
18
19 eventually kill it. The mechanism may involve damage to the cell membrane. Since
20
21 bacteria that persist are likely to have low energy pools, they are particularly liable to be
22
23 killed by PZA.
24
25
26
27
28
29

30 The natural route of infection of TB is via inhalation of bacilli-containing aerosols.
31
32 The bacilli settle in the deep lung, where they are phagocytized by alveolar
33
34 macrophages, ultimately resulting in pulmonary TB infection. Targeted delivery of anti-
35
36 TB therapies directly to infected lungs results in immediate contact of the drug with the
37
38 TB bacteria, leading to high local drug concentrations and rapid onset of killing action. A
39
40 smaller dose combined with the absence of first pass metabolism is expected to lead to
41
42 reduced systemic side effects and ultimately enhanced patient compliance to the
43
44 treatment, compared to the orally-delivered regimen. Particles deposit in the lung by
45
46 inertial impaction, sedimentation and diffusion [18, 19]. Large particles (aerodynamic
47
48 diameter, $d_a > 5 \mu m$) tend to deposit by impaction in the extra-thoracic cavities, smaller
49
50 particles ($d_a = 1-5 \mu m$) deposit deeper in the lungs by inertial impaction and
51
52 sedimentation, while very small particles ($d_a < 1 \mu m$) are driven by diffusion, mostly
53
54
55
56
57
58
59
60

1
2
3 remain suspended, and are ultimately exhaled. A number of anti-TB drugs have been
4 formulated in dry powder microparticles for pulmonary delivery, including capreomycin
5 [20, 21] and paraaminosalicylic acid [22]. Indeed, these studies indicated that direct
6 delivery to the lungs results in high local concentrations and reduced bacterial burden
7 compared to the same treatments delivered via other routes, offering the possibility of
8 both reduced doses and reduced systemic side effects. The delivery of antitubercular
9 drugs to the lungs has been reviewed thoroughly elsewhere [23, 24].
10
11
12
13
14
15
16
17
18
19

20 It is proposed that aerosol particles containing POA salts delivered to the lungs
21 (Figure 1a) in sizes that would facilitate peripheral deposition (Figure 1b) where
22 macrophage uptake (Figure 1c) would bring the drug proximal to the micro-organism will
23 enhance therapeutic effect (Figure 1d).
24
25
26
27
28
29

30 The novelty of the work described consists of: (a) The use of POA as a candidate
31 for tuberculosis therapy; (b) its preparation as a salt which is justified by a hypothesis
32 that has previously not been addressed and; (c) preparation of the salt as a particulate
33 dosage form to capitalize on local delivery to the lungs.
34
35
36
37
38
39

40 MATERIALS

41
42
43 POA was purchased from Sigma Aldrich, L-leucine was purchased from Fluka and
44 ammonium hydroxide was purchased from Fisher Scientific.
45
46
47
48

49 Nuclear magnetic resonance demonstrated the presence of stoichiometric 1:1
50 ratios of POA to leucine and ammonium ion in each of the salt forms. The weight
51 percentage by elemental analysis was within $\pm 0.4\%$, confirming the exact stoichiometric
52 ratios.
53
54
55
56
57
58
59
60

METHODS

Pyrazinecarboxylic acid (1.00 g, 8.05 mmol) and L-leucine (1.06g, 8.05 mmol) were suspended in water (50 mL). The reaction mixture was heated to 60 °C and stirred until the reaction mixture became clear. The solution was cooled to room temperature and the solvent was removed under vacuum. The resulting salt was collected and dried on high vacuum for an extensive period of time (1 week) to give the desired product as a white powder in quantitative yield (2.06 g).

Pyrazinecarboxylic acid (4.0 g; 32.2 mmol) was suspended in water (30 mL) and aqueous ammonium hydroxide (4.52 mL; 38.7 mmol) was added drop wise to the reaction mixture. The reaction was stirred for 30 minutes and a clear homogeneous solution was obtained. The solvent was removed under vacuum to provide a white solid. The resulting solid was suspended in methanol (50 mL) and stirred at room temperature for 2 hours to assist to remove the excess ammonium hydroxide. The final salt was collected by filtration and dried on high vacuum for an extensive period of time (1 week) to give final product as a white powder in quantitative yield (4.54 g).

Salt Characterization

¹H NMR: ¹H NMR spectra were recorded on a Bruker Avance DPX-300 (300 MHz) spectrometer. Around 5 mg of each salt was dissolved in 0.7 ml of an appropriate deuterated solvent (deuterated water for leucine salt and deuterated dimethyl sulfoxide for ammonium salt) and submitted immediately to NMR analysis. Chemical shifts are

1
2
3 reported in ppm relative to the reference signal and coupling constant (J) values are
4
5 reported in hertz (Hz).
6
7

8 **Elemental analysis:** Approximately 10 mg of each salt was analyzed by Atlantic
9
10 Microlab, Inc. (Georgia, US). The elements carbon, nitrogen, and hydrogen were
11
12 analyzed by combustion using automatic analyzers. All results are presented as percent
13
14 by weight determinations.
15
16

17 **Hot Stage Microscopy.** Samples were prepared and analyzed using a capillary melting
18
19 point apparatus (Mel-Temp II, Laboratory Devices, Inc., Holliston, MA). Each salt was
20
21 powdered and placed in thin-walled capillary tube (1 mm diameter, 10 cm height) in the
22
23 heating chamber of the melting point apparatus. In order to first determine the melting
24
25 point range, the initial melting experiment was run with the starting temperature at 25 °C
26
27 and ramping rate was set to ensure a steady increase of ~5 °C/min. For precise
28
29 measurements a second melting experiment was performed with the starting
30
31 temperature at 10 °C below the melting point range previously determined and a
32
33 ramping rate at 2 °C/min was employed.
34
35
36
37
38

39 Particle Manufacture

40
41
42 Aqueous solutions of the salts were prepared by dissolution in ultrapure water
43
44 (resistivity = 18.2 MΩ-cm, Barnstead NanoPure, Thermoscientific, Waltham, MA) at a
45
46 mass concentration of 10 mg/mL, with solutions having pH of 2.70 ± 0.02 and 4.56 ±
47
48 0.02 for POA-leu and POA-NH₄ respectively (SympHony, VWR, Radnor, PA). Solutions
49
50 were spray dried (Model B-290, Buchi, Falwil, Switzerland) in an open loop
51
52 configuration, with a two-fluid nozzle of inner and outer orifice diameters 0.7 and 1.5
53
54 mm, respectively. Ultra-high purity nitrogen was employed as the atomizing gas. The
55
56
57
58
59
60

1
2
3 aspirator was operated at 35 m³/hour capacity. The solution was introduced by a
4
5 peristaltic pump at a flow rate of 6.5 mL/min, while atomizing gas was adjusted to flow
6
7 rates between 439 – 1052 liters/hour. The inlet temperature was 140°C, corresponding
8
9 to an outlet temperature of 80°C. Powders were removed from the collection vessel
10
11 and stored in amber glass vials over desiccant at room temperature. Recovery was
12
13 determined gravimetrically with respect to nominal mass spray dried (400mg).
14
15
16

17 18 Particle Characterization

19
20
21 **Morphology:** Particle morphology after spray drying was evaluated by scanning
22
23 electron microscopy (Quanta 200, FEI, Hillsboro, OR). Powder was sampled onto an
24
25 adhesive carbon substrate mounted on an aluminum sample holder and sputter coated
26
27 with gold/palladium (Hummer Sputtering System, Anatech Ltd, Union City, CA) for a
28
29 period of 120 seconds. Images of POA salts were captured.
30
31
32

33
34 **X-Ray Powder Diffraction (XRPD):** POA alone, POA-NH₄ and POA-leu before and
35
36 after spray drying were evaluated (XRD-600, Shimadzu, Japan). Powder was loaded
37
38 into a glass sample holder, packed to uniform geometry and analyzed from 5-70° 2 θ at
39
40 an interval of 0.02° 2 θ with a dwell time at each step of 2 seconds without rotation, and
41
42 a slit arrangement of 1 degree for the divergence and scatter slits. X-ray beam source
43
44 was a copper anode operated at 45 kV and 40 mA.
45
46
47

48
49 **Thermal Analysis:** Two methods were employed to evaluate the powder thermal
50
51 properties. POA alone, POA-NH₄ and POA-leu before and after spray drying (denoted
52
53 hereafter as “SD”) were evaluated.
54
55
56
57
58
59
60

1
2
3 *Thermogravimetric analysis:* Salts were analyzed (TGA Q50, TA Instruments, New
4 Castle, DE) for moisture loss and thermal decomposition by placing in a platinum
5 sample pan and heating at a rate of 2°C/min from 20°-300°C and a sample mass of
6 approximately 5mg with nitrogen purge at 60 mL/min.
7

8
9
10
11
12 *Differential Scanning Calorimetry:* Samples were analyzed (Q200, TA Instruments, New
13 Castle, DE) for phase transitions in response to heating by placing in aluminum pans,
14 crimping and using a ramp rate of 5° C/min.
15
16
17
18
19

20
21 ***Residual Moisture Determination by Karl Fischer Titration:*** Powders were analyzed
22 after spray drying for water content by Karl Fischer titration on a Mettler Toledo V30
23 Compact Volumetric Karl Fischer Titrator using 3-5 mg per replicate (n=3).
24
25
26
27
28

29 ***Aerodynamic Particle Size Distribution (APSD):*** Mass median aerodynamic diameter
30 (MMAD) was determined by inertial impaction using a Next Generation Impactor (NGI)
31 (MSP Corporation, Minneapolis, MN). The impactor was operated with preseparator and
32 at a flow rate of 60 L/min, a standard practice for evaluating dry powder inhaler
33 performance [25]. Each of the spray dried POA salt powders (10 mg) was loaded into
34 #3 hydroxypropylmethylcellulose (HPMC) capsules (Quali-V, Qualicaps, Whitsett, NC)
35 and delivered (3x) to the impactor from a Cyclohaler dry powder inhaler (Plastiapae,
36 Osnago LC, Italy) which has a pressure drop of 16.4 mBar at 60 L/min [26]. Impactor
37 stages were coated with silicone oil to minimize particle bounce with the exception of
38 the micro-orifice collector plate. Samples were recovered from stages with deionized
39 water and solutions were assayed spectrophotometrically at a wavelength of 268nm
40
41
42
43
44
45
46
47
48
49
50
51
52
53
54
55
56
57
58
59
60

1
2
3 cumulative percent by mass of particles undersize against respective stage cutoff
4 diameter and applying a log-linear fit of two points on either side of 50% cumulative
5 mass [27] to identify the median. The geometric standard deviation was estimated from
6 the square root of the ratio of the particle size defined by the 84th percentile of the
7 distribution with respect to the particle size defined by the 16th percentile of the
8 distribution.
9

10
11
12
13
14
15
16
17
18 **Emitted dose:** Each of the POA salt powder aerosols was sampled through a glass
19 fiber filter using sampling apparatus B designated in USP <601> [25] operated at 60
20 L/min with 10mg capsules loaded as previously stated. Filter and apparatus interior
21 were washed and subsequently assayed by UV-Vis. Emitted dose was determined as a
22 percentage of emission from one actuation of a 10 mg capsule.
23
24
25
26
27
28
29

30
31 **Fine Particle Fraction:** Fine particle fraction (FPF < 4.46 μ m) can be presented as a
32 function of nominal (FPF_N) and emitted dose (FPF_{ED}). The nominal dose is that in the
33 capsule. The FPF_N is the ratio of mass collected on impactor stages 3 through the
34 micro-orifice collector with respect to the nominal dose expressed as a percentage. The
35 FPF_{ED} is the ratio of the mass collected on impactor stages 3 through the micro-orifice
36 collector with respect to the total mass delivered to the impactor including the inlet and
37 the preseparator expressed as a percentage.
38
39
40
41
42
43
44
45
46
47

48 **Antibacterial activity of POA salts.** The antibacterial effect of the POA salts were
49 tested *in vitro* on *Mtb* strain H37Rv (*Mtb* H37Rv) and Bacillus Calmette-Guerin (BCG,
50 attenuated *M bovis*), BCG does not have amidase and, therefore, does not convert
51 PZA to POA salt (Figure 1d). *Mtb* H37Rv and BCG was kept as a stock strain in liquid
52
53
54
55
56
57
58
59
60

1
2
3 nitrogen and serially transferred at weekly intervals to 7H9 Broth+ ADC(Becton
4 Dickinson.).
5
6

7
8 Experimental procedure:
9

10 Seven day cultures of *Mtb* H37Rv and BCG were grown in 7H9 broth (pH 6.2) and
11 inoculated at a1: 4 by volume in 30-ml screw cap universals. These cultures were
12 incubated for 60 days undisturbed. At the start of the experiment pH was adjusted to
13 5.6. using 1M sodium citrate. Samples were taken for viable count (T0). Antibacterial
14 drugs were added at concentrations of 150 mg/L of PZA, POA and each of the two
15 salts. Over a 21-day period of incubation at 37° C, weekly samples were taken and
16 viable counts were determined.
17
18
19
20
21
22
23
24
25

26
27 Viable counts: Samples were briefly ultrasonicated to disrupt cell aggregates. Ten fold
28 serial dilutions were made in water and 0.1 ml volume plated onto one-third segment of
29 7H11 agar+OADC (Becton Dickinson) medium plates. Plates were packed into
30 polyethylene bags and incubated for 3-4 weeks at 37°C before bacteria (colony forming
31 units, CFU). Colony counts were converted to log₁₀ cfu/mL. Four replicates samples
32 were evaluated and means and standard deviations calculated. All work was carried out
33 in Biological Containment Level 3 laboratory according to Health and Safety Act (1974)
34 and COSSH (2004) and are suitable for handling ACDP Hazard group 3 pathogens.
35
36
37
38
39
40
41
42
43
44

45
46 Statistics: T-test and ANOVA were performed to compare the means and the variances
47 between each of the treated and untreated groups. Statistical significance for both tests
48 was defined as p<0.05.
49
50
51
52
53
54
55
56
57
58
59
60

RESULTS

Salt Characterization

¹H NMR: Chemical shifts were determined for each of the salts. The POA-Leu chemical shifts appeared as follows: (300 MHz, D₂O) δ 9.10 (s, 1H), 8.66 (d, J = 6.0 Hz, 2H), 3.75 (m, 1H), 1.45 – 1.75 (m, 3H), 0.85 (m, 6H). The POA-NH₄ chemical shifts appeared as follows: (300 MHz, DMSO-d₆) δ 8.98 (s, 1H), 8.53 (s, 2H), 7.043 (br.s., 3H).

Elemental analysis: Elemental analysis for both salts correlate with the theoretical calculation of equimolar concentrations of POA and respective counterion, as shown in Table 1.

Preliminary Melting point determination: Melting point analysis revealed that the leucine salt decomposed at a temperature of 175°C while the ammonium salt melted at 181-183°C.

Particle Characterization

Recovery as a proportion of the initial mass after spray drying of small quantities of POA-leu was 39% and POA-NH₄ was 10%.

Particle Morphology: The POA-leu particles, shown in Figure 2a, appeared as collapsed hollow spheres with smooth surfaces and small pores. POA-NH₄ particles were mostly spherical with a corrugated surface, as depicted in Figure 2b. The geometric mean diameters were 3.7 ± 1.77 and 4.6 ± 1.87 μ m for POA-leu and POA-NH₄ respectively, as determined by image analysis (n=100).

X-Ray Powder Diffraction: XRPD data are shown in Figure 3. POA shows a primary peak at 27.69°, with modest but detectable peaks at other angles. POA-leu had

1
2
3 dominant peaks in order of intensity at 13.35, 24.36 and 30.57° 2 θ . POA-leu SD had
4
5 dominant peaks at 19.05, 19.74, and 27.61° 2 θ . POA-NH₄ had dominant peaks at
6
7 12.78, 15.54 and 19.90° 2 θ . POA-NH₄ SD had dominant peaks at 14.24, 19.72 and
8
9 27.52° 2 θ . Peaks were observed for leucine in order of peak intensity at 24.36, 30.56,
10
11 12.12 and 36.84° 2 θ . The intensity for the primary peak for the POA alone was much
12
13 greater than any of peaks of the salt powders.
14
15
16

17 ***Thermal Analysis***

18
19
20
21 *Thermogravimetric analysis:* Thermograms are shown in Figure 4. POA-leu displayed a
22
23 bimodal TGA profile, with onset of the first event occurring at 110°C and culminating at
24
25 180°C, and the second event occurring from 180°C to 250°C, as shown in Figure 4a.
26
27 Figure 4b shows the behavior of POA and leucine alone as a reference for the inflection
28
29 observed in the salt thermogram. The TGA curve for POA-NH₄ was marked by a single
30
31 event occurring from 100°C to the loss of all mass at 157°C as shown in Figure 4c.
32
33 TGA data from the spray dried material closely match those of the starting material,
34
35 each having little residual solvent. Loss of POA begins at 110°C and culminates at
36
37 180°C. Figure 4d compares the profile of POA against both salts. There was no
38
39 evidence for the presence of moisture at the limit of detection of this method in either
40
41 powder as would ordinarily be seen as a distinct feature on the thermogram
42
43 representing mass loss at temperatures slightly below 100° up to 150°C depending on
44
45 the extent of binding (free or bound).
46
47
48
49
50
51

52
53 *Differential Scanning Calorimetry:* Figure 5 depicts the DSC endotherms generated
54
55 from an evaluation of salts before and after spray drying. It is evident that the melting
56
57
58
59
60

1
2
3 point of POA (223 °C) was lowered in the salts (POA-leu ~200 °C, POA-NH₄, ~180 °C)
4
5 to approximately the same extent both before and after spray drying. Consequently,
6
7 there does not appear to be a significant effect of spray drying on the melting point.
8
9

10
11 **Residual Moisture Determination by Karl Fischer Titration:** POA-leu and POA-NH₄
12
13 spray dried powders had an average moisture content of 0.37% ± 0.06 and 0.66% ±
14
15 0.43 respectively.
16
17

18
19 **Aerodynamic Particle Size Distribution:** Figure 6 shows the APSDs of the two salt
20
21 forms. POA-leu particles exhibited a MMAD of 3.29 ± 0.05 μm and a GSD of 1.91 ± 0.2
22
23 (n=3), FPF_N of 44% and FPF_{ED} of 61%. MMAD for POA-NH₄ particles was 5.4 μm
24
25 (GSD 1.83), with FPF_N of 34% and FPF_{ED} of 40%.
26
27
28

29
30 **Emitted dose:** was 71.7 ± 3.4% and 69.8 ± 2.8% for POA-leu and POA-NH₄,
31
32 respectively (n=6).
33
34

35
36 **Antibacterial activity of POA salts:** The antimicrobial effect of POA salts are shown in
37
38 Figure 7. The effects of POA in various forms on the growth of *Mtb* (Figure 7a), strain
39
40 H37Rv and attenuated *Mycobacterium bovis* (BCG, Figure 7b) are shown. At all times
41
42 following the initiation of the experiment the drug treatments were significantly effective
43
44 in killing *Mtb H37Rv* in comparison to the untreated control group. At 14 and 21 days
45
46 the POA salt and PZA treated groups were statistically more effective in killing *MTb*
47
48 *H37Rv* than the POA alone. Throughout the experiment PZA was statistically similar in
49
50 effect to untreated control in terms of BCG. At all times following initiation of the
51
52 experiment POA salts and POA alone were statistically more effective in killing BCG
53
54
55
56
57
58
59
60

1
2
3 than either PZA or untreated control groups. At 14 and 21 days the POA salts were
4
5 statistically more effective ($p < 0.05$) than POA alone.
6
7

8 9 **DISCUSSION**

10
11 Elemental analysis and melting behavior of the reaction products indicated that the
12
13 process successfully generated salts. Elemental analysis confirmed the identification of
14
15 the salts, with the theoretical and experimental values within the margin of error. Melting
16
17 point determination demonstrated a single melt phenomenon rather than separate
18
19 effects due to the independent components of the construct. The melting point values
20
21 were addressed more accurately and in comparison with POA in the subsequent
22
23 thermal analysis.
24
25
26
27
28

29
30 Given the thermal profile of POA a low outlet temperature with respect to
31
32 decomposition temperature was targeted while atomization parameters were chosen
33
34 based on prior experience with spray drying other small molecules. [28]
35
36

37 **Particle Morphology:** Morphologically, the POA-leu particles resemble previously
38
39 reported particles with moderate leucine content, possibly due to high initial droplet
40
41 surface saturation during drying [29]. This results in earlier shell formation and larger,
42
43 less dense particles. Such particles generally are more dispersible than smaller, denser
44
45 particles.
46
47
48

49
50 POA-NH₄ particles are corrugated in appearance with a hollow sphere, low
51
52 density morphology. These particles exhibited an aerodynamic diameter that was
53
54 greater than their geometric diameter. Given the aerodynamic diameter can be
55
56 approximated as the product of the square root of the particle density and the geometric
57
58
59
60

1
2
3 diameter [25], this suggests insufficient deaggregation. Spray drying yield of the
4 ammonium salt (as a proportion of the nominal mass of 400mg) was low relative to the
5 leucine (10% and 39%, respectively, for the same mass) and could be improved with
6 further optimization. Wall losses do not scale proportionately to mass being spray dried.
7
8 Increasing the mass spray dried would significantly increase yield. The POA-NH₄
9 particles were more adherent to the spray drying collection vessel and would also
10 experience significant increase in yield at high mass output since the vessel surfaces
11 would be saturated. Consequently, recovery may be improved by increasing the batch
12 size.
13
14
15
16
17
18
19
20
21
22
23

24
25 ***X-Ray Powder Diffraction:*** Data displayed distinct peaks for POA and both salts,
26 before and after spray drying. The two salts had distinct and different crystalline peaks
27 as bulk materials. The peak data for POA matched phase identification data for POA
28 (PDF 00-27-1888)[30]. The two spray dried materials appear to have similar diffraction
29 patterns, sharing the dominant peak location with that of POA. The POA-leu spectra
30 show peaks throughout the spectrum that can be attributed as POA and leucine where
31 they have been combined and POA in the ammonium salt for which the ion cannot be
32 studied in the solid state. The lower intensity of the peaks in the salts with respect to
33 POA alone indicate, in light of examining similar quantities of powder accounting for the
34 proportion of the components, the potential for amorphous content. In addition, the
35 variation in intensity of peaks within the spectrum that may be assigned to POA ,
36 particularly in the initial salts with respect to the POA alone may be an indication of
37 polymorphism in the starting materials which has been observed by others for related
38
39
40
41
42
43
44
45
46
47
48
49
50
51
52
53
54
55
56
57
58
59
60

1
2
3 salts [31]. However, the peaks in the spray dried material are more closely aligned both
4
5 in angle and intensity to POA alone.
6
7

8
9 **Thermogravimetric analysis:** Thermogravimetric analysis shows differences in loss
10
11 between the two salts as synthesized. The profile of POA-leu corresponds to the
12
13 individual profiles for L-leucine and POA. POA-NH₄ showed onset of loss at a lower
14
15 temperature than POA itself, while POA-leu and POA had similar onset temperatures.
16
17

18
19 **Differential Scanning Calorimetry:** POA showed decomposition at 223°C which is
20
21 consistent with published values [32]. POA salts show similar thermal behavior before
22
23 and after spray drying, indicating the process was not detrimental to the material. Melt
24
25 peak onset occurred at temperatures slightly below those observed in the capillary
26
27 method which is to be expected given the sensitivity of this method compared with
28
29 capillary melting point method used to screen the salts immediately after manufacture.
30
31
32

33
34 **Residual Moisture Determination by Karl Fischer Titration:** Moisture content as
35
36 determined by Karl Fischer is supported by thermogravimetric analysis curves which do
37
38 not show noticeable mass loss corresponding to unbound water.
39
40

41
42 **Aerodynamic Particle Size Distribution:** Aerodynamic size is within appropriate
43
44 range for lung deposition. POA-leu SD exhibited a smaller MMAD than POA-NH₄ SD,
45
46 potentially due to the lower density afforded by the initial surface saturation of the
47
48 leucine salt as previously described. Smaller particles can be achieved through an
49
50 optimized experimental design carefully modifying spray drying parameters. Methods for
51
52 decreasing particle size include increasing the mass flow ratio between the atomizing
53
54
55
56
57
58
59
60

1
2
3 gas and the liquid feed and decreasing the concentration of dissolved solids in the
4
5 solution. Emitted dose for both powders was sufficient for efficient use in other studies.
6
7

8
9 ***Antibacterial activity of POA:*** As expected PZA had a high antibacterial effect on Mtb
10
11 H37Rv but not on BCG, and POA was bactericidal for both strains, with higher effect on
12
13 BCG than Mtb H37Rv. Interestingly, both POA salts were more bactericidal on the two
14
15 bacterial strains than pure POA which supports the hypothesis that the salt form
16
17 increases the killing effect. The bacteria were held under static conditions for up to 60
18
19 days, then pH changed to acid conditions to ensure the bactericidal action of PZA and
20
21 POA. The two logarithm reduction achieved by the salts with respect to untreated
22
23 control and benefits seen with respect to PZA and POA alone would be an enormous
24
25 advantage when translated to the multiple drug regimen standard of care described
26
27 earlier (EHRZ).
28
29
30
31
32

33
34 In order to understand the significance of the outcome of the antibacterial activity
35
36 studies the effects of pH on the efficacy of POA can be explored further. The Zhang
37
38 hypothesis, described earlier, is supported by experimental evidence. [16, 17]
39
40 Paradoxically, after the initial deamination within the bacilli, the POA produced leaves
41
42 the bacilli fairly readily. However, after the POA has re-entered the cell, it is eliminated
43
44 by means of an efflux pump. Either POA traverses the cell membrane with comparative
45
46 ease (as postulated after the deamination step) or it only traverses it with great difficulty
47
48 (as postulated to account for its lethal accumulation within the cell). To get over this
49
50 logical problem, it has been postulated that first that the charged POA molecule cannot
51
52 easily pass through the cell membrane. After deamination, the $-NH_3$ molecule turns to
53
54 ammonium ($NH_4.OH$) on contact with cell water which then combines with the POA to
55
56
57
58
59
60

1
2
3 form POA-NH₄. This uncharged salt should pass through the cell membrane with ease.
4
5 In an acid environment, the dissociated POA ion from the salt would be protonated and
6
7 would NOT diffuse through the cell membrane to accumulate within the cell.
8
9

10
11 An explanation for the appearance of PZA inactivity in culture was explained by
12
13 McDermott & Tompsett in 1954 [33]. In these experiments, Tween-albumin or oleic acid-
14
15 albumin liquid media were adjusted by addition of NaOH or HCl to a range of pH values
16
17 between pH 4.5 and pH 8.0. It was clear that there was a great change in the MIC over
18
19 the range of pH 6.0-5.5. The effect of pH on the activity of other potential anti
20
21 tuberculosis drugs used in first line therapy is also relevant.
22
23

24
25 There are two possible explanations for the pH of active tuberculosis lesions
26
27 being acidic. Firstly, because inflammation accompanied by anoxia tends to produce
28
29 acid conditions by the accumulation of lactic acid [34] and secondly because counts of
30
31 viable bacilli in sputum show that PZA treatment, given without any other anti-
32
33 tuberculosis drugs in studies of early bactericidal activity, is bactericidal during the initial
34
35 14 days of treatment [35]. On average, 97% of the bacilli were killed in this study and
36
37 there was no apparent alteration in the speed of the bactericidal action once it had
38
39 started at about day 2. Thus, the great majority of the bacterial population that is being
40
41 sampled in sputum is at a sufficiently acid pH for the PZA given in treatment to be
42
43 clearly bactericidal. Since peak plasma concentrations are about 30 µg/ml PZA [36],
44
45 these lesions must have a pH of less than 6.0 for the achievable PZA concentration in
46
47 the lesions to be above the MIC. Multiplication of *M. tuberculosis* must be occurring
48
49 because large numbers of bacilli are being excreted from the lungs in sputum.
50
51
52
53
54
55
56
57
58
59
60

1
2
3 Salts of POA were more effective in an in vitro evaluation of action against two
4 mycobacteria. It has been demonstrated here that these salts can be prepared as
5 respirable dry powders suitable for further evaluation in an animal model.
6
7
8
9

10
11 The immediate priorities for future work are further optimization of the spray
12 drying process, performance of studies to evaluate the in vivo efficacy and tolerability of
13 the POA salts in animals.
14
15
16
17
18
19
20
21
22
23
24
25
26
27

28 **ACKNOWLEDGMENTS**

29
30
31
32 We are grateful to Mr. J. Todd Ennis for assistance in obtaining X-ray powder diffraction
33 data. Some of the data in this paper was presented in abstract at the American
34 Association of Pharmaceutical Scientists Annual Meeting held in San Antonio, TX
35 during November 2013.
36
37
38
39
40
41
42
43
44
45
46
47
48
49
50
51
52
53
54
55
56
57
58
59
60

REFERENCES

1. World Health Organization, *Fact Sheet No. 104* 2015.
2. Fox, W., *Whither short-course chemotherapy?* Br J Dis Chest, 1981. **75**(4): p. 331-57.
3. *Essentially of Pyrazinamide Workshop*. in *Stop TB Partnership Working Group on New Drugs*. 2011. Bethesda, MD.
4. Mitchison, D.A., *Role of individual drugs in the chemotherapy of tuberculosis*. Int J Tuberc Lung Dis, 2000. **4**(9): p. 796-806.
5. Lu, P., et al., *Pyrazinoic acid decreases the proton motive force, respiratory ATP synthesis activity, and cellular ATP levels*. Antimicrob Agents Chemother, 2011. **55**(11): p. 5354-7.
6. Cole, S.T., *Microbiology. Pyrazinamide--old TB drug finds new target*. Science, 2011. **333**(6049): p. 1583-4.
7. Shi, W., et al., *Pyrazinamide inhibits trans-translation in Mycobacterium tuberculosis*. Science, 2011. **333**(6049): p. 1630-2.
8. Kjellsson, M.C., et al., *Pharmacokinetic evaluation of the penetration of antituberculosis agents in rabbit pulmonary lesions*. Antimicrob Agents Chemother, 2012. **56**(1): p. 446-57.
9. Matthews, J., *IX. Pyrazinamide and isoniazid used in the treatment of pulmonary tuberculosis*. Am Rev Respir Dis., 1960. **81**: p. 348-351.
10. McKenzie, D., et al., *The effect of nicotinic acid amide on experimental tuberculosis of white mice*. J Lab Clin Med., 1948. **33**: p. 1249-1253.
11. Solotorovsky, M., et al., *3rd. Pyrazinoic acid amide; an agent active against experimental murine tuberculosis*. Proc Soc Exp Biol Med., 1952. **79**(4): p. 563-565.
12. Yeager, R.L., W.G. Munroe, and F.I. Dessau, *Pyrazinamide (aldinamide) in the treatment of pulmonary tuberculosis*. Am Rev Tuberc, 1952. **65**(5): p. 523-46.
13. McCune, R. and R. Tompsett, *Fate of Mycobacterium tuberculosis in mouse tissues as determined by the microbial enumeration technique. I. The persistence of drug-susceptible tubercle bacilli in the tissues despite prolonged antimicrobial therapy*. J Exp Med. , 1956. **104**: p. 737-762.
14. East African/British Medical Research Councils, *Controlled clinical trial of short-course (6-month) regimens of chemotherapy for treatment of pulmonary tuberculosis*. The Lancet, 1972. **299**(7760): p. 1079-1085.
15. Konno, K., F.M. Feldmann, and W. McDermott, *Pyrazinamide susceptibility and amidase activity of tubercle bacilli*. Am Rev Respir Dis, 1967. **95**(3): p. 461-9.
16. Zhang, Y. and D. Mitchison, *The curious characteristics of pyrazinamide: a review*. Int J Tuberc Lung Dis, 2003. **7**(1): p. 6-21.
17. Scorpio, A., et al., *Characterization of pncA mutations in pyrazinamide-resistant Mycobacterium tuberculosis*. Antimicrob Agents Chemother, 1997. **41**(3): p. 540-3.
18. Scheuch, G., et al., *Clinical perspectives on pulmonary systemic and macromolecular delivery*. Adv Drug Del Rev., 2006. **56**: p. 996-1008.
19. Smola, M., T. Vandamme, and A. Sokolowski, *Nanocarriers as pulmonary drug delivery systems to treat and to diagnose respiratory and non respiratory diseases*. Int J Nanomedicine., 2008. **3**: p. 1-19.
20. Garcia-Contreras, L., et al., *Inhaled large porous particles of capreomycin for treatment of tuberculosis in a guinea pig model*. Antimicrob Agents Chemother., 2007. **51**: p. 2830-2836.
21. Fiegel, J., et al., *Preparation and in vivo evaluation of a dry powder for inhalation of capreomycin*. Pharmaceutical Research, 2008. **25**(4): p. 805-11.

- 1
2
3
4
5
6
7
8
9
10
11
12
13
14
15
16
17
18
19
20
21
22
23
24
25
26
27
28
29
30
31
32
33
34
35
36
37
38
39
40
41
42
43
44
45
46
47
48
49
50
51
52
53
54
55
56
57
58
59
60
22. Tsapis, N., et al., *Direct lung delivery of para-aminosalicylic acid by aerosol particles*. Tuberculosis, 2003. **83**: p. 379-385.
 23. Muttill, P., C. Wang, and A.J. Hickey, *Inhaled drug delivery for tuberculosis therapy*. Pharmaceutical Research, 2009. **26**(11): p. 2401-16.
 24. Misra, A., et al., *Inhaled drug therapy for treatment of tuberculosis*. Tuberculosis (Edinb), 2011. **91**(1): p. 71-81.
 25. Convention, U.S.P., *U.S. Pharmacopeia National Formulary 2011: USP 34 NF 292011*: United States Pharmacopeial.
 26. Srichana, T., G.P. Martin, and C. Marriott, *Dry powder inhalers: The influence of device resistance and powder formulation on drug and lactose deposition in vitro*. European Journal of Pharmaceutical Sciences, 1998. **7**(1): p. 73-80.
 27. International Standards Organization, *Anaesthetic and respiratory equipment*, in *Nebulizing systems and components*2009.
 28. Chuck, R.J. and U. Zacher, *Spray drying an aqueous solution of ammonium nicotinate;heating aftertreatment*, 2002, Google Patents.
 29. Vehring, R., *Pharmaceutical Particle Engineering via Spray Drying*. Pharmaceutical Research, 2008. **25**(5): p. 999-1022.
 30. JCPDS--International Centre for Diffraction Data American Society for Testing Materials, *Powder Diffraction File: Inorganic and organic*2001: JCPDS International Centre for Diffraction Data.
 31. Prasad, K.D., et al., *Differential CocrySTALLIZATION Behavior of Isomeric Pyridine Carboxamides toward Antitubercular Drug Pyrazinoic Acid*. Crystal Growth & Design, 2015. **15**(2): p. 858-866.
 32. Lewis, M.W., *Preparation of pyrazinoic acid*, 1954, Google Patents.
 33. McDermott, W. and R. Tompsett, *Activation of pyrazinamide and nicotinamide in acidic environments in vitro*. Am Rev Tuberc, 1954. **70**(4): p. 748-54.
 34. von Ardenne, M. and W. Kruger, *Local tissue hyperacidification and lysosomes*. Front Biol, 1979. **48**: p. 161-94.
 35. Jindani, A., C.J. Dore, and D.A. Mitchison, *Bactericidal and sterilizing activities of antituberculosis drugs during the first 14 days*. Am J Respir Crit Care Med, 2003. **167**(10): p. 1348-54.
 36. Ellard, G.A., *Absorption, metabolism and excretion of pyrazinamide in man*. Tubercle, 1969. **50**(2): p. 144-158.

FIGURE LEGENDS

1
2
3
4
5
6
7
8
9
10
11
12
13
14
15
Figure 1. The role of POA salt (POA-leucine and POA-NH₄) in elevating the bactericidal activity of PZA, and bypassing resistance. a) POA salts are manufactured and aerosolized into microparticles. b) Inhaled microparticles are deposited in the alveolar, c) where the microparticles are phagocytosed by macrophages infected with *M. tuberculosis*. d) Inside macrophages, microparticle dissolves and the POA salt modulates local pH increasing the activity of PZA.

16
17
18
Figure 2. Scanning electron micrographs depicting particles resulting from the spray drying of a) POA-leu salt and b) POA-NH₄.

19
20
21
22
Figure 3. X-ray powder diffraction patterns for a) pyrazinoic acid (POA) and L-leucine and b) pyrazinoate salts before and after spray drying.

23
24
25
26
27
Figure 4. Thermogravimetric analysis thermograms for a) POA-leu before and after spray drying, b) POA-leu salt as compared to POA and L-leucine, c) POA-NH₄ before and after spray drying, and d) a comparison of POA to both salts.

28
29
30
Figure 5. Differential scanning calorimetry curves for POA and pyrazinoate salts before and after spray drying.

31
32
33
34
Figure 6. Aerosol particle size distribution depicted as mass deposition per impactor stage for spray dried pyrazinoate salts (n=3, mean ± SD)

35
36
37
38
39
40
41
42
43
44
45
46
47
48
49
50
51
52
53
54
55
56
57
58
59
60
Figure 7. Bacterial growth inhibition of a) *Mycobacterium tuberculosis* strain H37Rv and b) *Mycobacterium bovis* strain BCG by pyrazinamide, POA and POA-salts as compared to untreated control evaluated over a period of 21 days (n=4, mean ± SD). ANOVA and t-test, statistical significance (p<0.05) * compared to untreated control, **compared to POA alone.

Figure 1:

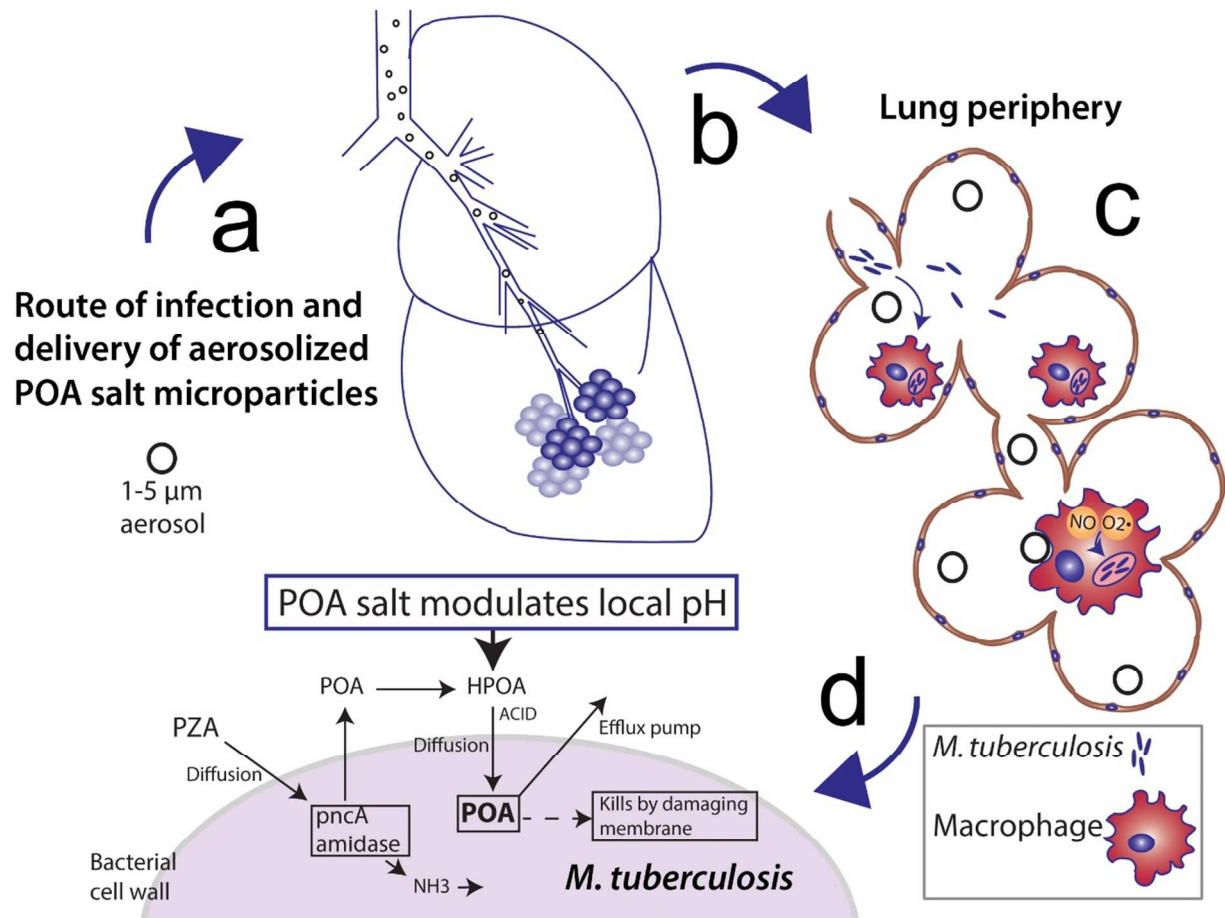


Figure 2. SEM

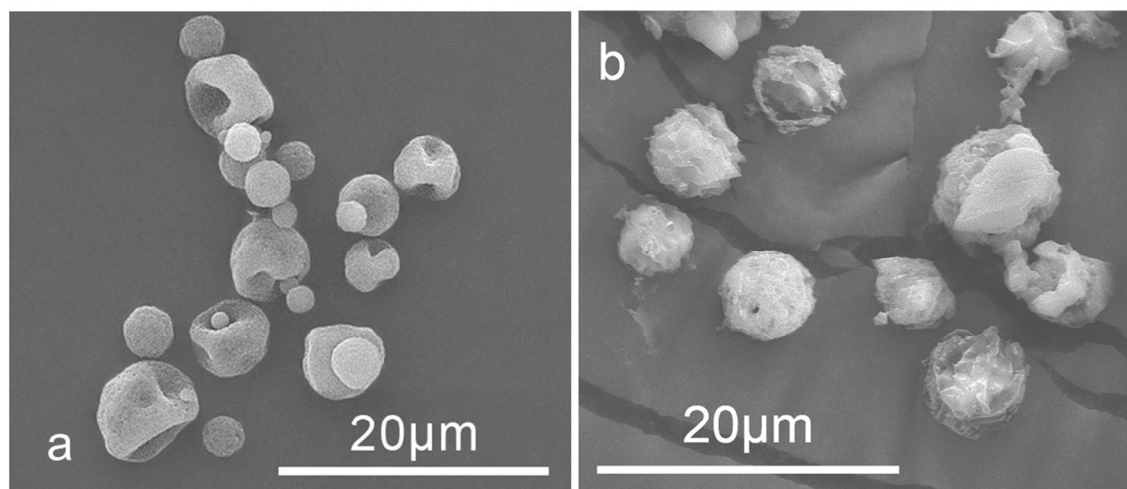


Figure 3. XRPD

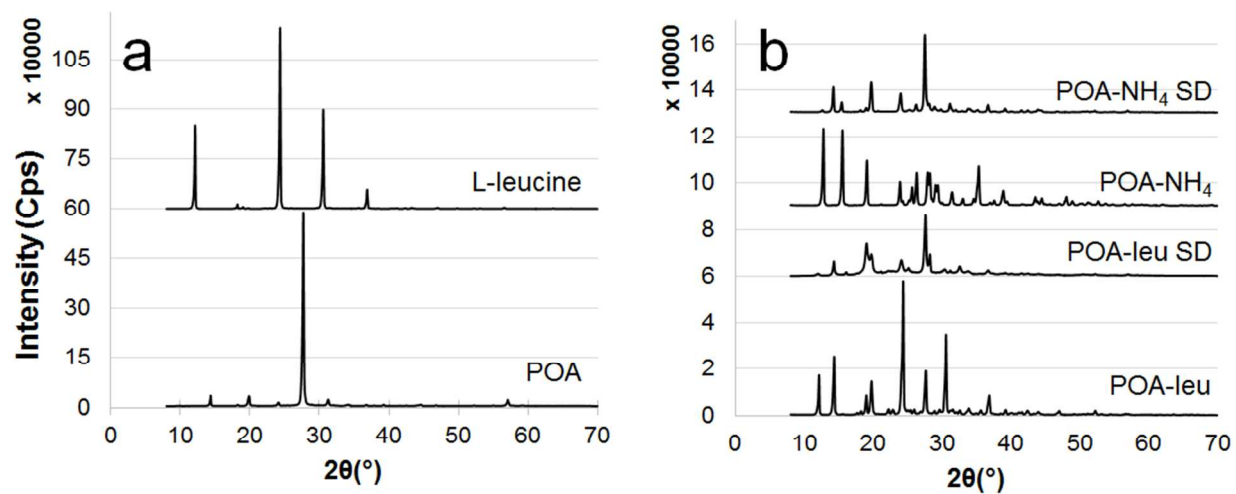


Figure 4. TGA

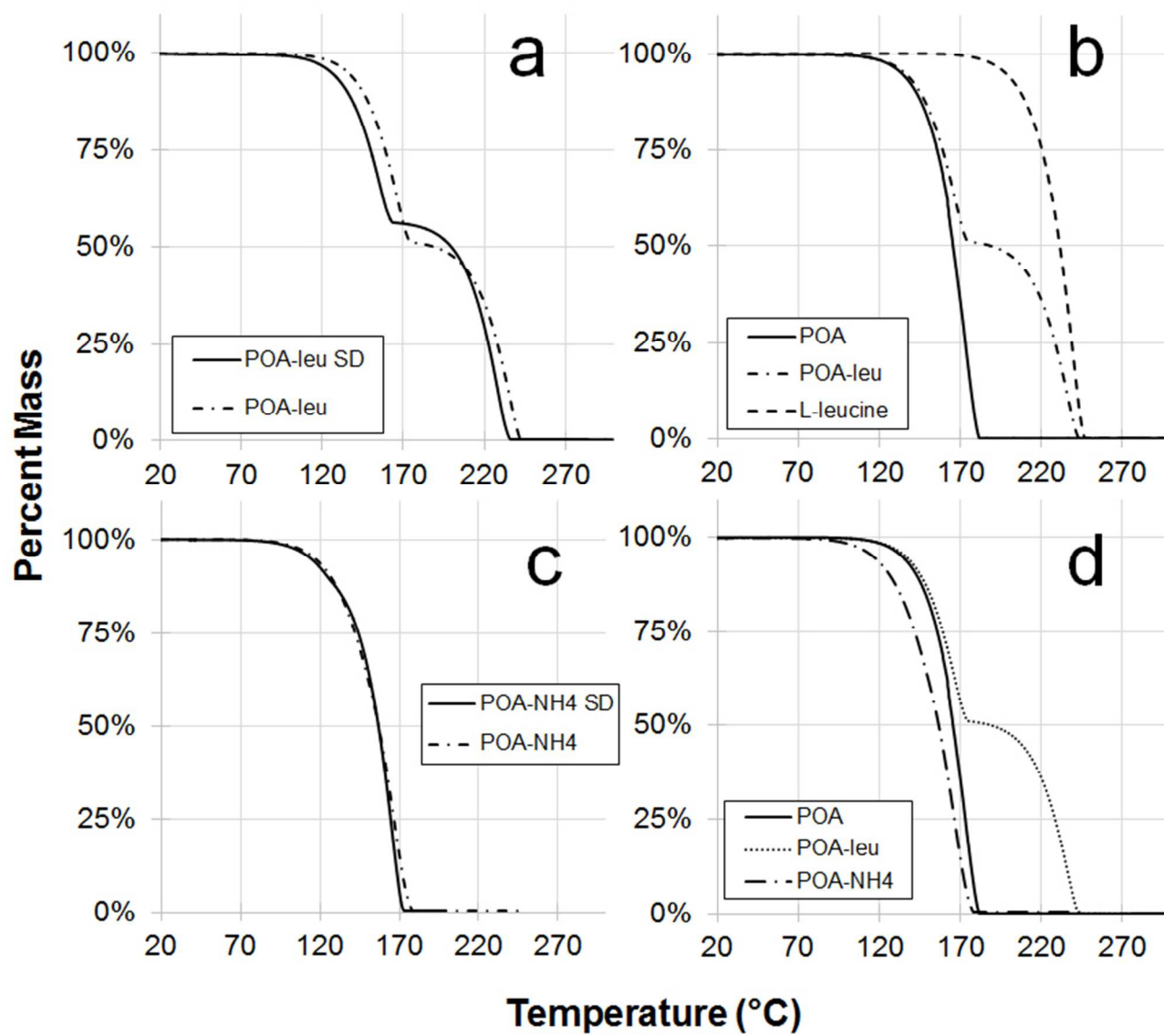


Figure 5. DSC

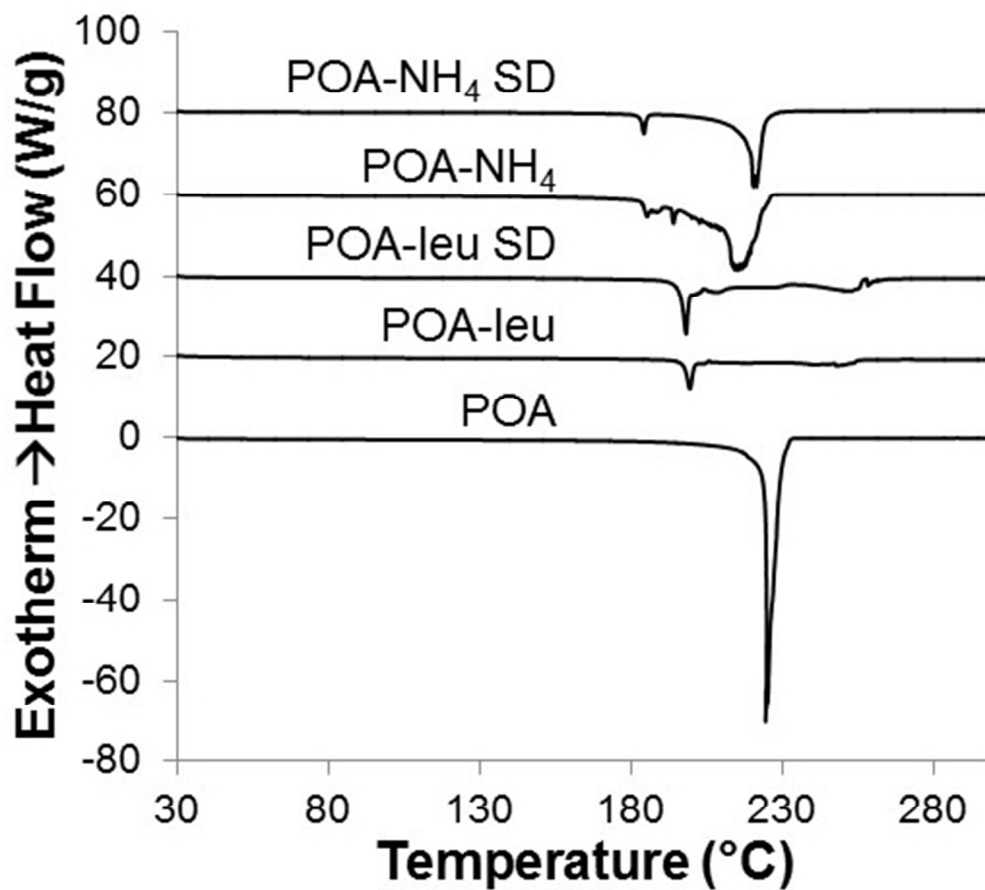


Figure 6. APSD

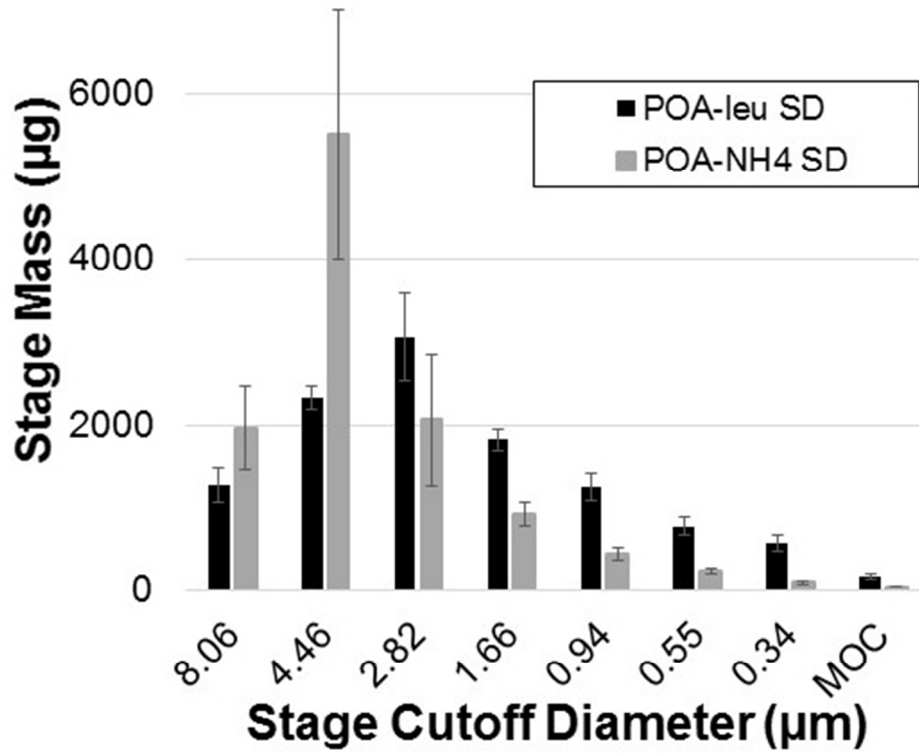


Figure 7. MIC

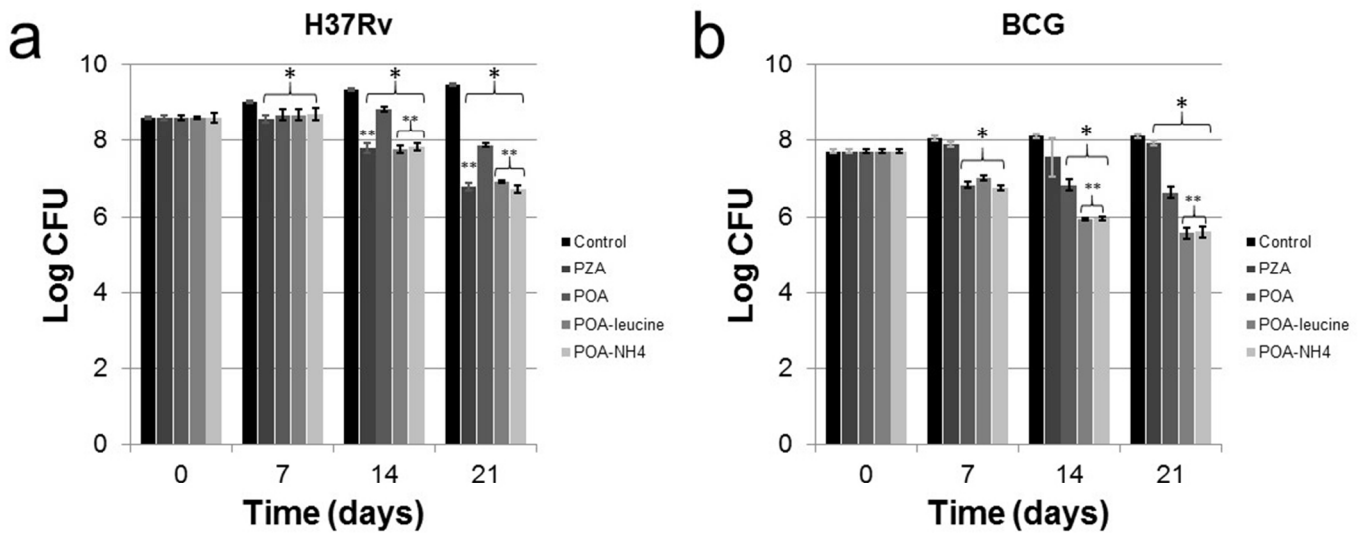


Table 1. Elemental Analysis

POA-leu		
Element	Theoretical	Experimental
C	51.76	51.90
H	6.71	6.94
N	16.46	16.16

POA-NH4		
Element	Theoretical	Experimental
C	42.55	42.81
H	5.00	5.05
N	29.77	29.79

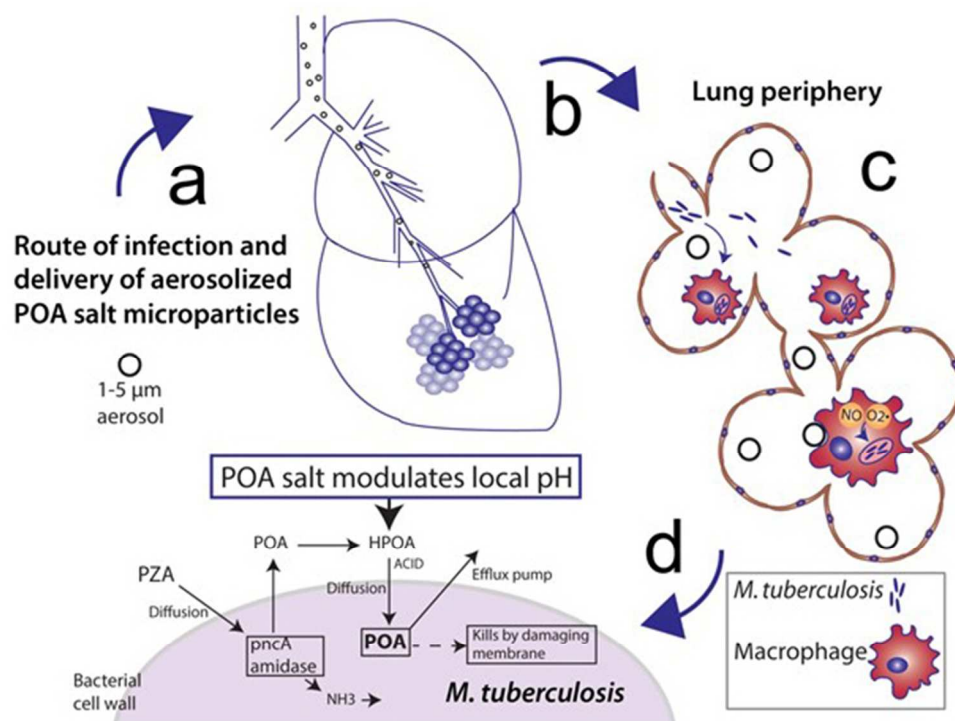


Figure 1. The role of POA salt (POA-leucine and POA-NH₄) in elevating the bactericidal activity of PZA, and bypassing resistance. a) POA salts are manufactured and aerosolized into microparticles. b) Inhaled microparticles are deposited in the alveolar, c) where the microparticles are phagocytosed by macrophages infected with *M. tuberculosis*. d) Inside macrophages, microparticle dissolves and the POA salt modulates local pH increasing the activity of PZA.

67x51mm (240 x 240 DPI)

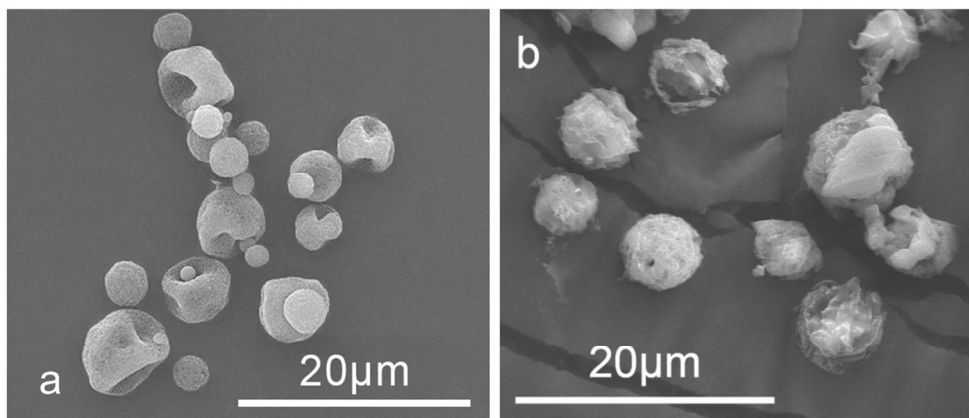
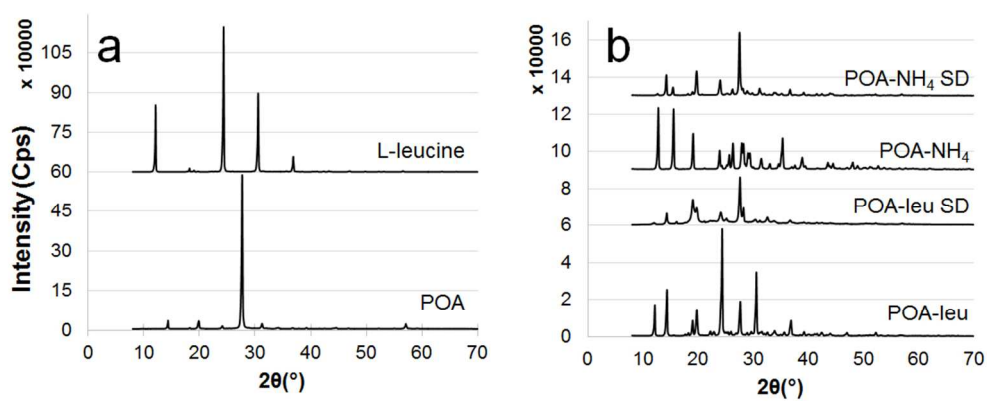


Figure 2. Scanning electron micrographs depicting particles resulting from the spray drying of a) POA-leucine salt and b) POA-ammonium salt.
135x58mm (240 x 240 DPI)



X-ray powder diffraction patterns for a) pyrazinoic acid (POA) and L-leucine and b) pyrazinoate salts before and after spray drying.
393x164mm (72 x 72 DPI)

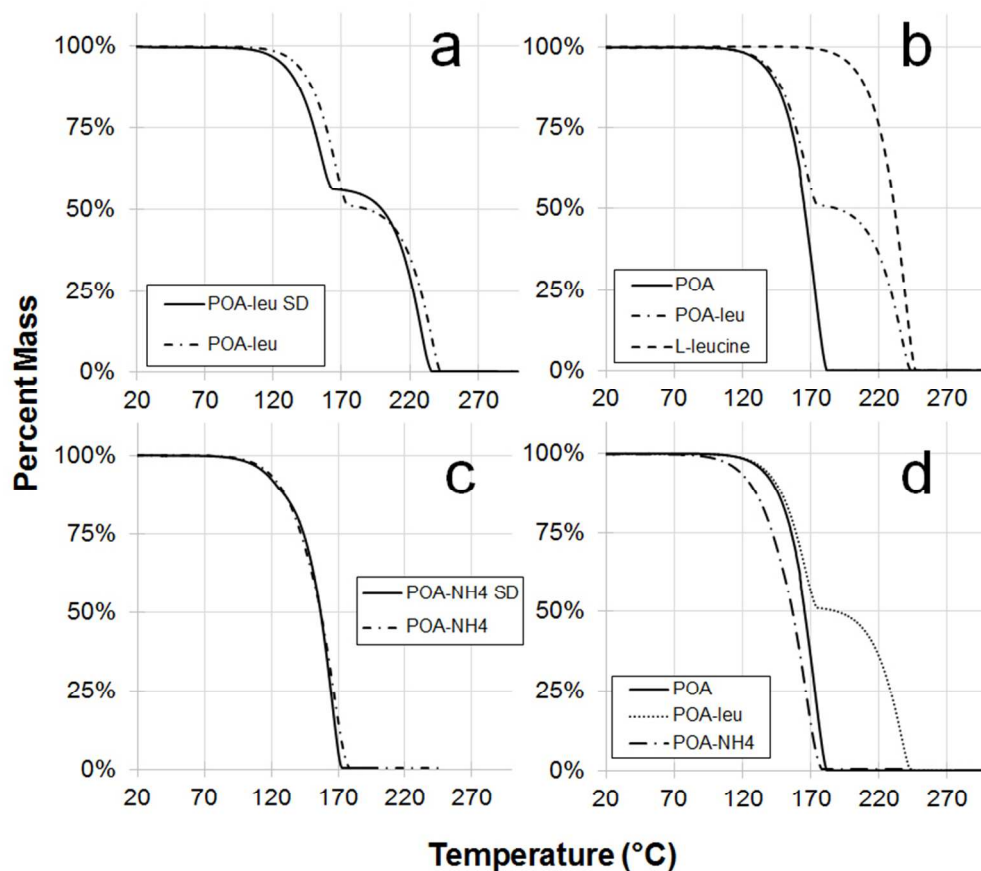


Figure 4. Thermogravimetric analysis thermograms for a) POA-leucine before and after spray drying, b) POA-leucine salt as compared to pyrazinoic acid and L-leucine, c) POA-NH₄ before and after spray drying, and d) a comparison of pyrazinoic acid to both salts.
91x83mm (240 x 240 DPI)

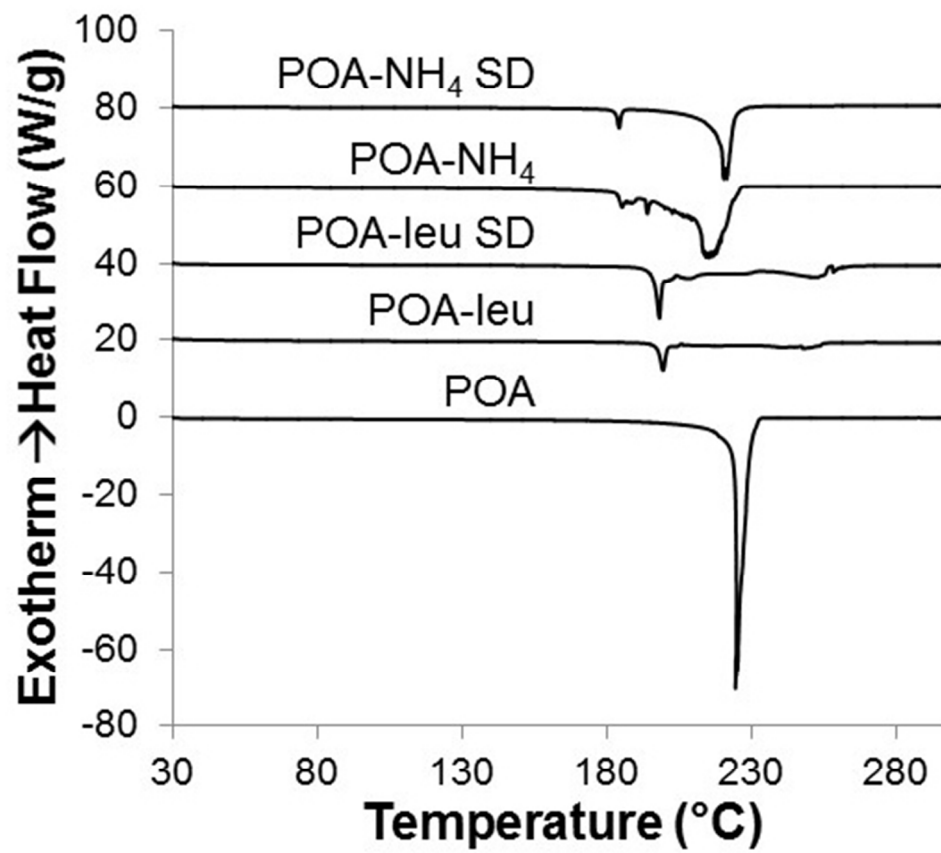


Figure 5. Differential scanning calorimetry curves for pyrazinoic acid and pyrazinoate salts before and after spray drying.
57x50mm (240 x 240 DPI)

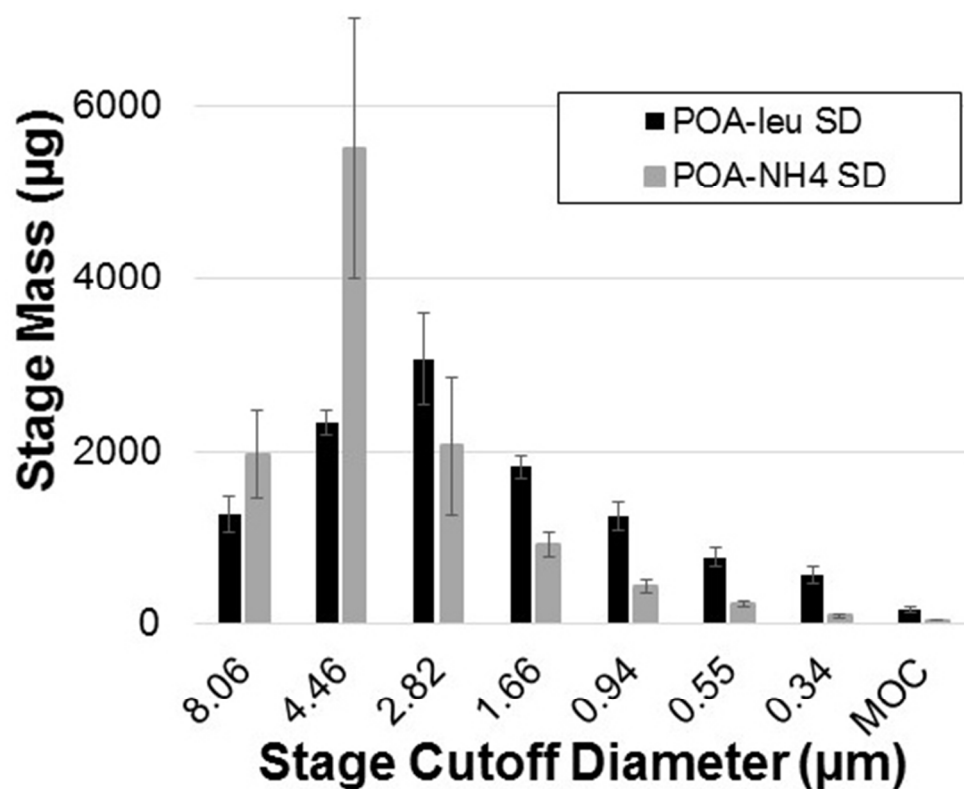
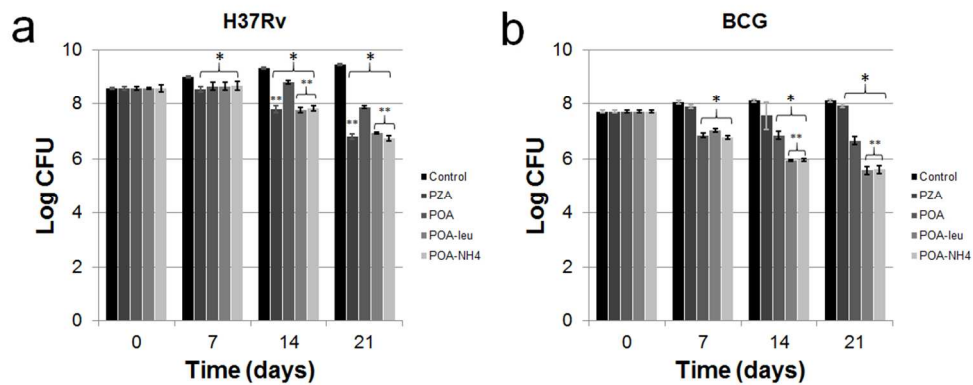


Figure 6. Aerosol particle size distribution depicted as mass deposition per impactor stage for spray dried pyrazinoate salts (n=3, mean \pm SD) 56x46mm (240 x 240 DPI)



Bacterial growth inhibition of a) *Mycobacterium tuberculosis* strain H37Rv and b) *Mycobacterium bovis* strain BCG by pyrazinamide, POA and POA-salts as compared to untreated control evaluated over a period of 21 days (n=4, mean \pm SD). ANOVA and t-test, statistical significance ($p < 0.05$) * compared to untreated control, **compared to POA alone.
403x162mm (72 x 72 DPI)